

## Original Article

# Triptolide induces immunogenic cell death in cervical cancer cells via ER stress and redox modulation

Ziwen Zheng<sup>1,2</sup>, Yamei Chen<sup>2</sup>, Chao Wang<sup>2</sup>, Ling Li<sup>3</sup>, Buzhen Tan<sup>1</sup>

<sup>1</sup>The Second Affiliated Hospital, Jiangxi Medical College, Nanchang University, Nanchang 330006, Jiangxi, China;

<sup>2</sup>Department of Gynecological Oncology, Jiangxi Cancer Hospital, Jiangxi Cancer Center, Nanchang 330029,

Jiangxi, China; <sup>3</sup>Department of Gynecological Oncology, Jiangxi Maternal and Child Health Hospital, Nanchang 330006, Jiangxi, China

Received October 18, 2024; Accepted December 26, 2024; Epub January 15, 2025; Published January 30, 2025

**Abstract:** Cervical cancer remains a significant global health burden, particularly in developing countries, despite advances in screening and prevention. Novel therapeutic strategies are urgently needed to improve outcomes for patients with advanced or metastatic disease. Triptolide (TL), a key component of the Chinese herb *Tripterygium wilfordii*, has shown potent anticancer effects in various malignancies. In this study, we investigated the anticancer effects of TL on cervical cancer cells *in vitro* and *in vivo*, focusing on its ability to induce immunogenic cell death (ICD). TL exhibited potent cytotoxicity, inhibited proliferation, induced apoptosis, and suppressed tumor growth in cervical cancer models. Mechanistically, TL induced ICD in cervical cancer cells, as evidenced by the calreticulin (CRT) exposure on the cell surface and the release of HMGB1 and ATP. TL-induced CRT exposure was mediated by endoplasmic reticulum (ER) stress, as demonstrated by the upregulation of ATF3 and the activation of oxidative stress and immune pathways. Oral administration of TL significantly inhibited tumor growth in a cervical cancer xenograft model, without overt toxicities. These findings highlight the potential of TL as a novel immunotherapeutic agent for cervical cancer and warrant further investigation into its clinical translation. The combination of TL with immune checkpoint inhibitors or other immunotherapies may provide a promising strategy to enhance the efficacy of cervical cancer treatment while minimizing adverse effects.

**Keywords:** Triptonide, cervical cancer, immunogenic cell death, ER stress, redox modulation, immunotherapy

## Introduction

Cervical cancer (CC) continues to pose a substantial global health challenge, particularly affecting women in developing nations [1, 2]. Despite advances in screening, prevention, and treatment, the mortality rate associated with cervical cancer has remained relatively stable [3]. This stagnation is largely attributed to cases diagnosed at advanced stages with distant metastasis, where current therapeutic strategies often fail to achieve curative outcomes [4]. Postoperative recurrence prevention and patient survival improvement are commonly addressed through clinical chemotherapy regimens; however, these treatments often result in severe adverse effects [5]. As a result, the search for effective natural therapeutics with minimal side effects remains a crucial focus of current research efforts.

Diterpene triepoxides, Triptolide (TL) and Triptonide (TN), are principal extracts from *Tripterygium wilfordii* Hook, a traditional Chinese medicinal plant [1, 6]. TL, recognized as the essential bioactive constituent, features a hydroxyl group at C-14 and exhibits a spectrum of pharmacological effects, including immunosuppression, anti-inflammation, and anticancer properties [6, 7]. However, the clinical application of TL is limited by poor water solubility and high toxicity (especially hepatotoxicity and nephrotoxicity) [8]. Despite these challenges, recent studies have demonstrated the potent anticancer activity of TL in various cancers, including breast, prostate and colorectal malignancies [9-11]. In CC, TL has been shown to disrupt copper homeostasis and induce copper-dependent apoptosis by regulating the XIAP/COMMD1/ATP7A/B axis, as well as inhibit the RTK/Akt-mTOR pathway, thereby impairing CC cell growth and survival [12, 13].

Preclinical research has demonstrated that TL exerts multifaceted anticancer effects, including the suppression of tumor cell proliferation, induction of apoptosis, inhibition of angiogenesis, and modulation of immune responses [14]. Cai et al. found that co-administration of TL with IFN- $\gamma$  induced cytotoxic CD8<sup>+</sup> T lymphocyte activation, showing a synergistic effect on effective tumor suppression and enhancing anti-tumor immunity in triple-negative breast cancer [15].

Moreover, TL has demonstrated significant potential in overcoming chemotherapy resistance and enhancing the effectiveness of standard chemotherapeutic regimens, underscoring its viability as an innovative anticancer therapeutic [16-18]. These findings highlight the promising potential of TL as a novel anti-cancer agent. However, the influence of TL on cervical neoplasia and the intricate molecular pathways involved remain largely unexplored. Given its potent anticancer effects and the pressing need for innovative therapeutic strategies in cervical cancer, we hypothesize that TL may serve as a potential therapeutic agent for this malignancy. A comprehensive investigation into the mechanisms of action, toxicity attenuation, and clinical translation of TL in cervical cancer is therefore warranted. Such studies may pave the way for the development of TL-based therapies that can effectively combat cervical cancer while minimizing adverse effects.

Immunogenic cell death (ICD) has emerged as a promising strategy to enhance the efficacy of cancer immunotherapy by eliciting a tumor-specific immune response [13]. The exposure of damage-associated molecular patterns (DAMPs), such as calreticulin (CRT), high mobility group box 1 (HMGB1), and adenosine triphosphate (ATP), on the surface or their release from dying cancer cells is essential for ICD [19]. These DAMPs interact with specific receptors on antigen-presenting cells (APCs) to activate immune cells and trigger a cytotoxic T lymphocyte-mediated anti-tumor response [20]. Recent research has identified celastrol (Celt), a compound derived from *Tripterygium wilfordii* Hook, as effective not only in inducing ICD but also in inhibiting PD-L1 through the down-regulation of MAPK1 expression. This study elucidates the anti-tumor properties of Celt in clear

cell renal cell carcinoma (ccRCC) by promoting ICD [21]. This indicates that other extracts from *Tripterygium wilfordii* Hook could potentially trigger ICD in CC.

The capacity of TL to provoke ICD in cervical cancer cells and its subsequent effects on immunotherapy remain insufficiently explored. Given the pressing demand for innovative treatments for advanced cervical cancer, we propose that TL may induce ICD in these cells by instigating ER stress, thereby acting as a potential ICD inducer for immunotherapy in this malignancy. TL has been documented to influence ER stress and reactive oxygen species (ROS), and this study uniquely integrates these effects with ICD. Specifically, our research seeks to elucidate how ER stress induced by TL, in conjunction with ROS generation, prompts the release of critical ICD markers, such as DAMPs, thereby activating anti-tumor immune responses. This mechanism underscores the immunomodulatory potential of TL in cancer therapy and enhances our understanding of its distinctive role in activating ICD through ER stress and oxidative stress pathways. This study will investigate TL's capability to induce ICD in cervical cancer cells through comprehensive *in vitro* and *in vivo* experiments, assessing its viability as an immunotherapeutic agent for advanced cervical cancer.

### Materials and methods

#### *Ethics*

The research adhered to the ethical guidelines established by the Declaration of Helsinki. The animal studies were performed following the National Institutes of Health's standards for laboratory animal welfare and received approval from the Institutional Animal Care and Use Committee and the Medical Ethics Committee of Jiangxi Cancer Hospital (ID: 2023ky097).

#### *Reagents and antibodies*

Triptonide (TL, purity > 98%) was obtained from Sigma-Aldrich (SMB00325), and details regarding its dissolution or dilution were described in our previous study [35]. Cell culture reagents were procured from Gibco. The following primary antibodies were used: HMGB1 (Abcam, ab18256), CRT (Thermo Fisher Scientific, PA1-902A), GAPDH (Cell Signaling Technology, 21-

## Triptonide induces ICD in cervical cancer

18), ATF3 (Abcam, ab207434), IRE1 $\alpha$  (Sigma-Aldrich, I6785).

### *Cell lines and culture conditions*

The cervical carcinoma cell lines HT-3 (human) and U14 (mouse) were procured from the Shanghai Institute for Biological Science's Cell Bank. These lines were chosen for their relevance in cervical cancer research. HT-3 cells, derived from human cervical cancer, are useful for studying molecular pathways and treatments, while U14 cells, derived from mouse models, were used in vivo to study tumor growth and immune responses. These cells were cultivated in Dulbecco's Modified Eagle Medium supplemented with 4.5 g/L glucose, 10% fetal bovine serum, and 100 U/mL of penicillin, 100  $\mu$ g/mL of streptomycin. The cell cultures were maintained at 37°C in a humidified environment with a 5% CO<sub>2</sub> atmosphere. To ensure purity, regular screenings for mycoplasma and other microbial contaminants were conducted, confirming the absence of such pollutants. Additionally, to verify their authenticity, STR profiling of the cell lines was systematically carried out triannually.

### *Animal experiments*

Female BALB/c juvenile mice, aged 5 weeks, were sourced from the Laboratory Animal Center of the Shanghai Institutes for Biological Sciences, Chinese Academy of Sciences. The mice were housed in a controlled, pathogen-free environment with free access to food and water. They were maintained under a 12-hour light-dark cycle at ambient temperatures between 20-22°C. Anesthesia was administered via intraperitoneal injection of ketamine at a dosage of 200 mg/kg prior to experimental interventions. Following the conclusion of the experiments, euthanasia was carried out humanely utilizing a chamber designed for carbon dioxide-induced euthanasia.

### *Assessment of cellular viability*

Cell viability was assessed using the Dojindo Cell Counting Kit-8 (Beyotime, C0037). In summary, cells were allocated into 96-well plates at  $5 \times 10^3$  cells per well and subjected to varying doses of TL for 24, 48, or 72 hours. Post-treatment, 10  $\mu$ L of CCK-8 reagent was added to each well, and the cells were incubated for 2 hours at 37°C. Absorbance was measured at

450 nm using a Bio-Rad microplate reader [22].

### *Colony formation assay*

For colony formation assessment, cells were plated in 6-well plates at 500 cells per well and exposed to TL for 24 hours. After treatment, cells were cultured for 14 days in fresh media. Resultant colonies were fixed with paraformaldehyde (4%), stained with crystal violet (0.1%), and enumerated under an Olympus inverted microscope [22].

### *EdU-based proliferation assay*

Cell proliferation was quantified using the Click-iT EdU Alexa Fluor 488 Imaging Kit (Invitrogen) according to the manufacturer's guidelines. Cells were plated on coverslips within 24-well plates and treated with TL for 24 hours. Afterward, the cells were incubated with EdU (10  $\mu$ M) for 2 hours, fixed, and permeabilized. Following staining with the Click-iT mixture and Hoechst 33342, images were captured using fluorescence microscopy.

### *Analysis of cell cycle progression*

Flow cytometric techniques were employed to delineate cell cycle phases. Post 24-hour TL exposure, cells were harvested and preserved in 70% ethanol at 4°C overnight. After fixation, cells were washed with PBS, stained with a PI/RNase solution (BD Biosciences) for 30 minutes at ambient temperature, and subsequently analyzed via a BD FACSCalibur cytometer.

### *Detection of apoptotic cells*

Apoptotic events were identified using Roche's In Situ Cell Death Detection Kit, employing the TUNEL method. Cells were plated on coverslips and treated with TL for 24 hours. After treatment, cells were fixed with 4% paraformaldehyde and permeabilized with 0.1% Triton X-100. The TUNEL mixture was then applied to the cells and incubated for an hour at 37°C in the dark, followed by DAPI staining. Apoptotic cells were quantified with an Olympus fluorescence microscope.

### *Assessment of ROS levels*

ROS generation was quantified with Abcam's cellular ROS assay kit, following the provided protocol. Initially, cells were cultured in six-well

## Triptonide induces ICD in cervical cancer

plates for 24 hours, then treated with TL for 10 hours. Post-treatment, cells incubated with DCFH2-DA dye for 30 minutes at 37°C. A BD flow cytometer was utilized to measure the resultant fluorescence intensity.

### *Immunofluorescence for CRT detection*

Cervical carcinoma cells were grown on coverslips, then fixed using 4% paraformaldehyde and permeabilized with 0.2% Triton X-100. Subsequent to blocking, cells were incubated overnight at 4°C with a primary antibody targeting CRT (Abcam, ab91654). The following day, cells were treated with a fluorophore-conjugated secondary antibody for 1 hour at room temperature. Nuclei were stained with 0.2 mg/mL DAPI, and fluorescence signals were captured using a confocal microscope to analyze CRT localization and expression.

### *Evaluation of antitumor activity in vivo*

U14 cells ( $5 \times 10^6$  cells per mouse) suspended in a 1:1 ratio of DMEM and Matrigel (50  $\mu$ L each) were injected subdermally into the upper right flank of 5-week-old female BALB/c mice. Tumor volumes typically reached around 100  $\text{mm}^3$  within three weeks, at which point the mice were randomly assigned to two groups. The treatment group received daily intragastric doses of Triptonide (10 mg/kg), based on prior studies and preliminary experiments [9, 23], while the control group was given an equivalent volume of saline over 21 consecutive days. Tumor dimensions were measured using calipers, and tumor volume was calculated using the formula:  $(\text{length} \times \text{width}^2)/2$ . Daily tumor growth rate ( $\text{mm}^3/\text{day}$ ) was calculated by monitoring changes in tumor volume throughout the treatment period [24].

### *Western blot analysis*

Cellular proteins were isolated using a lysis buffer designed for immunoprecipitation, enhanced with phenylmethanesulfonyl fluoride and a phosphatase inhibitor blend (P002, NCM Biotech). Protein concentrations were quantified using a bicinchoninic acid (BCA) assay. Proteins were then segregated via SDS-PAGE and transferred to 0.2- $\mu$ m PVDF membranes (Millipore). The membranes were incubated in 5% non-fat milk in TBS for 90 minutes, followed by over-

night incubation at 4°C with primary antibodies. Post-TBST washes, membranes were incubated with secondary antibodies for 60 minutes at ambient temperature. Bands were detected using an ECL substrate (E411-04, Vazyme) and imaged on an ImageQuant LAS 4000 Mini System, with quantification performed via ImageJ.

### *Transcriptome sequencing*

RNA was extracted from neoplastic tissues using RNAisoPlus (TaKaRa). Its integrity and concentration were appraised with a NanoDrop2000 spectrophotometer. Primers were sourced from Accurate Biology. cDNA synthesis was executed using Oligo dT (18T) and Evo M-MLV RTase Mix, following the manufacturer's protocol. RT-qPCR was carried out with SYBR Green PCR Master Mix on a 7500 Fast Real-time PCR System. GAPDH served as the normalization reference, and the  $2^{-\Delta\Delta C_t}$  method was applied for amplification curve analysis.

### *Bioinformatics analysis*

Differentially expressed genes (DEGs) were identified using the DESeq2 R package (version 1.30.1). Following probe annotation, a  $\log_2$  transformation was employed to achieve a distribution closer to normality. Criteria for DEG selection included an absolute  $\log_2(\text{Fold Change})$  greater than 1, a  $p$ -value below 0.01, and a baseMean exceeding 5. DEGs were visualized using heat maps, constructed by the ggplot2 package (version 3.4.1). Pathway enrichment of DEGs was analyzed with the aid of GSEABase (version 0.4-7), ReactomePA (version 1.34.0), and GseaVis (version 0.0.5). Gene Set Enrichment Analysis (GSEA) parameters were set as follows: nPerm at 10,000, pvalueCutoff at 0.2, and pAdjustMethod as BH. Gene Ontology (GO) analysis was conducted on genes meeting the following conditions: baseMean over 5,  $\log_2\text{FoldChange}$  above 1, and a  $p$ -value under 0.01, with both pvalueCutoff and qvalueCutoff set at 0.05.

### *Statistical analysis*

Data were analyzed using the Statistical Package for the Social Sciences (SPSS) version 16.0 (IBM, Chicago, IL, USA). Data were expressed as the mean  $\pm$  SD for samples with a

minimum count of three ( $n \geq 3$ ). Statistical significance among various groups was determined using one-way ANOVA followed by the LSD test. For the analysis of differences between two groups, Student's t-test was used. Data are presented using GraphPad Prism 8.0. A significant threshold was set at  $P$ -values less than 0.05. Significance levels were denoted as: \* $P < 0.05$ , \*\* $P < 0.01$ , and \*\*\* $P < 0.001$ .

### Results

#### *Triptonide exerted potent cytotoxicity to cervical cancer cells*

To evaluate the cytotoxic effects of TL on cervical cancer cells, we treated the cervical cancer cell lines HT-3 (human) and U14 (mouse) with various concentrations of TL (5-500 nM) for 72 h. The CCK-8 assay revealed that TL significantly reduced the viability of both HT-3 and U14 cells in a dose-dependent manner, with IC50 values of 26.77 nM and 38.18 nM, respectively (**Figure 1A**). Furthermore, the colony formation assay demonstrated that TL treatment markedly suppressed the clonogenic ability of HT-3 and U14 cells in a dose- and time-dependent manner (**Figure 1B**). Collectively, these results indicate that TL exerts potent cytotoxicity against cervical cancer cells.

#### *Triptonide inhibited the proliferation of cervical cancer cells*

To further investigate the anti-proliferative effects of TL on cervical cancer cells, we performed the EdU incorporation assay and cell cycle analysis. Treatment with TL (10-50 nM) for 48 h significantly reduced the percentage of EdU-positive nuclei in both HT-3 and U14 cells in a dose-dependent manner (**Figure 2A**), indicating that TL suppresses the proliferation of cervical cancer cells. As cell cycle progression is crucial for cancer cell proliferation, we next examined the impact of TL on cell cycle distribution using PI staining and flow cytometry. In TL-treated HT-3 and U14 cells, the percentages of cells in the G0/G1 and G2/M phases were markedly increased, while the percentage of cells in the S phase decreased (**Figure 2B**). Statistical analysis of cell cycle distribution by integrating five independent PI-FACS experiments revealed that TL induced a dose-dependent G1-S cell cycle arrest in both cell lines

(**Figure 2B**). Collectively, these findings demonstrate that TL inhibits the proliferation of cervical cancer cells by inducing G1-S cell cycle arrest.

#### *Triptonide induced apoptosis and reactive oxygen species (ROS) production in cervical cancer cells*

Given that TL reduced cell viability, induced growth arrest, and inhibited proliferation in cervical cancer cells, we next investigated its effects on apoptosis. TL treatment significantly increased the percentage of TUNEL-positive nuclei in a dose-dependent manner in both HT-3 and U14 cells (**Figure 3A**), indicating that TL induces apoptosis in cervical cancer cells. Since ROS production is often associated with apoptosis, we measured intracellular ROS levels using the DCFH-DA probe. TL treatment led to a significant increase in DCFH-DA fluorescence intensity in both HT-3 and U14 cells (**Figure 3B**), suggesting that TL promoted ROS generation in cervical cancer cells. To further confirm the pro-apoptotic effects of TL, we performed Annexin V-FITC/PI staining and flow cytometry analysis. TL treatment (10-50 nM) dose-dependently increased the percentage of Annexin V-positive cells in both HT-3 and U14 cells (**Figure 3C**), corroborating that TL induces apoptosis in cervical cancer cells. Therefore, TL efficiently induces both apoptosis and ROS production in cervical cancer cells.

#### *Triptonide suppressed the growth of human cervical cancer xenografts in nude mice*

To investigate the *in vivo* anti-cervical cancer activity of TL, we established a HeLa cell xenograft model in nude female mice. When the tumor volume reached approximately 100 mm<sup>3</sup>, the mice were administered either TL (10 mg/kg, daily by gavage for 21 days) or vehicle control (saline). The tumor growth curve revealed that TL treatment significantly inhibited the growth of HeLa xenograft tumors compared to the control group (**Figure 4A**). Moreover, the estimated daily tumor growth rate (mm<sup>3</sup>/day) was significantly lower in TL-treated mice compared to the control group (**Figure 4B**). Six weeks after the first gavage of TL, the mice were humanely euthanized, and tumor tissues were collected for volume and weight measurements. Xenograft tumors in the

## Triptonide induces ICD in cervical cancer

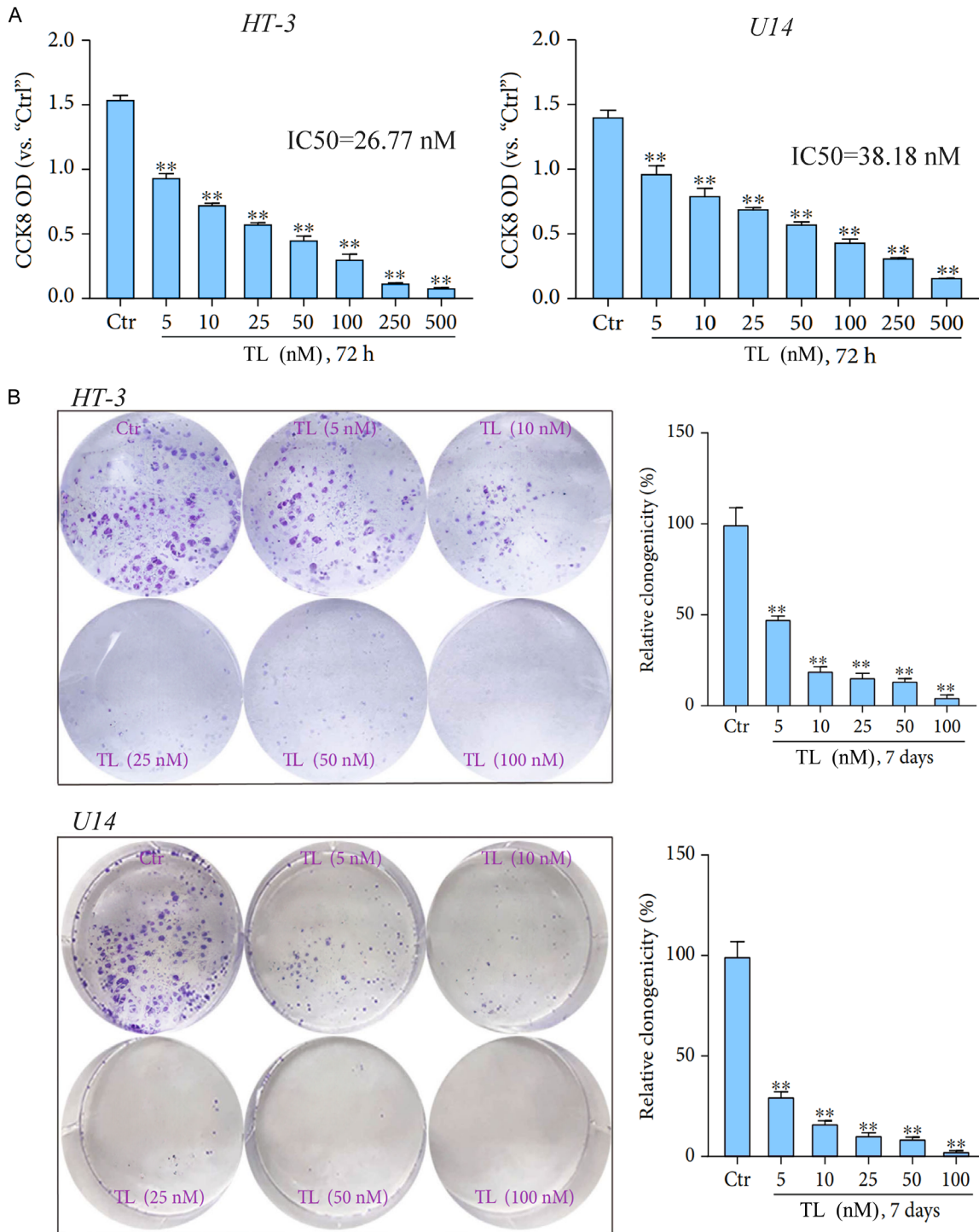


**Figure 1.** Triptonide exerted potent cytotoxicity on cervical cancer cells. A. HT-3 and U14 cells were exposed to various concentrations of Triptonide (TL) or vehicle control for 72 h, and cell viability was assessed using the CCK-8 assay. The half-maximal inhibitory concentration (IC<sub>50</sub>) was determined to be 26.77 nM for HT-3 and 38.18 nM for U14 cells. B. Colony formation assay of HT-3 and U14 cells treated with TL or vehicle control for 14 days. Data are presented as the percentage of relative clonogenicity, in the form of mean  $\pm$  SD of at least five independent experiments. "Ctr" represents the vehicle control group (0.1% DMSO). \*\*P < 0.01, compared to "Ctr".

TL group were markedly smaller than those from the vehicle control group (**Figure 4C**).

Notably, tumor weights did not differ significantly between the two groups throughout the

## Triptonide induces ICD in cervical cancer

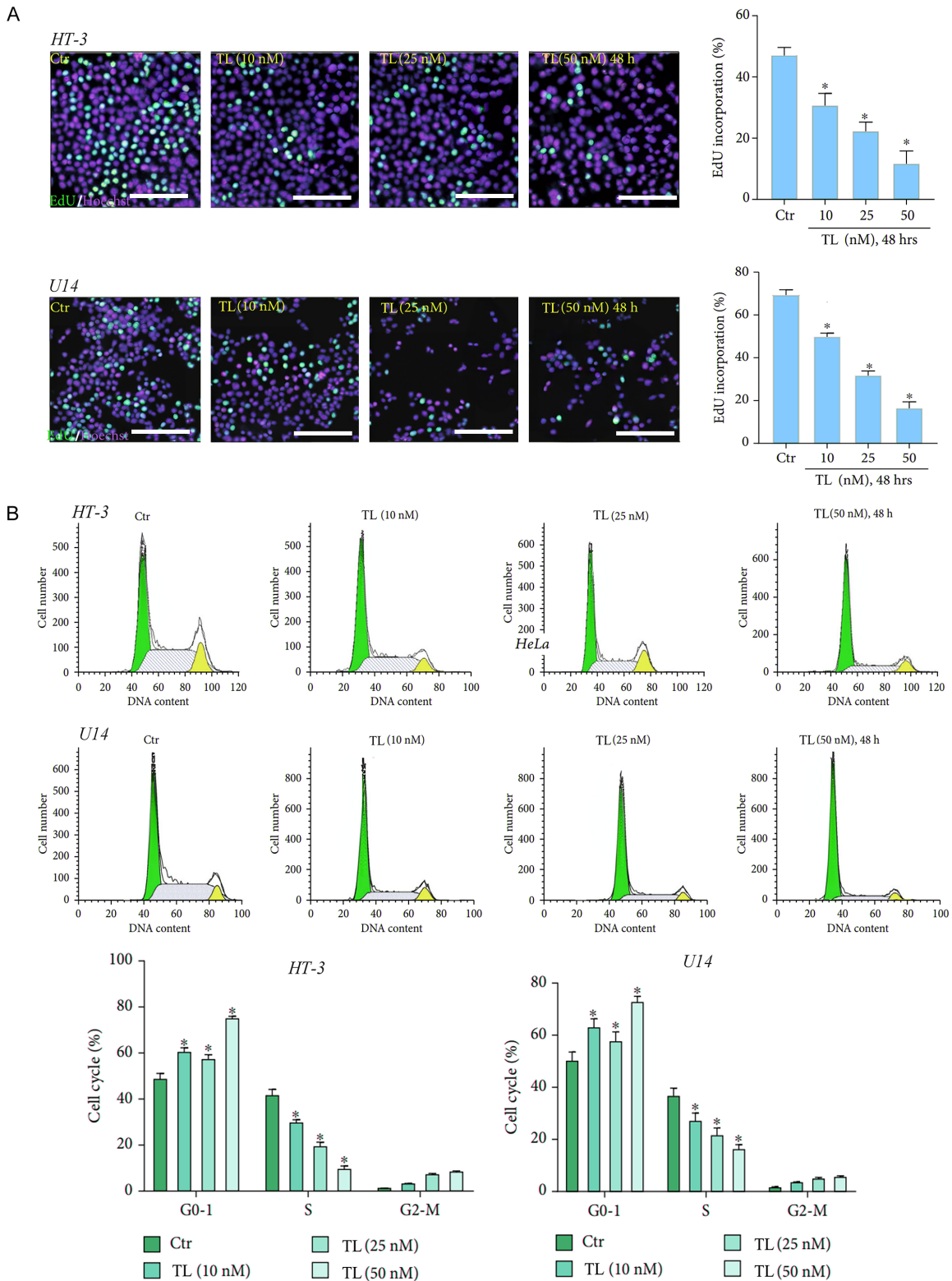


**Figure 2.** Triptonide inhibited the proliferation of cervical cancer cells by inducing G1-S cell cycle arrest. A. EdU incorporation assay of HT-3 and U14 cells treated with TL (10, 25, and 50 nM) for 48 h. Scale bar, 400  $\mu$ m. The percentage of EdU-positive cells (green) among Hoechst-stained nuclei (blue) was quantified. B. Cell cycle analysis of HT-3 and U14 cells treated with TL using PI staining and flow cytometry. The histograms show the distribution of cells in G0/G1, S, and G2/M phases. Data are presented as the mean  $\pm$  SD of five independent experiments. \*P < 0.05, compared to the control group "Ctr". Scale bar, 100  $\mu$ m.

## Triptonide induces ICD in cervical cancer

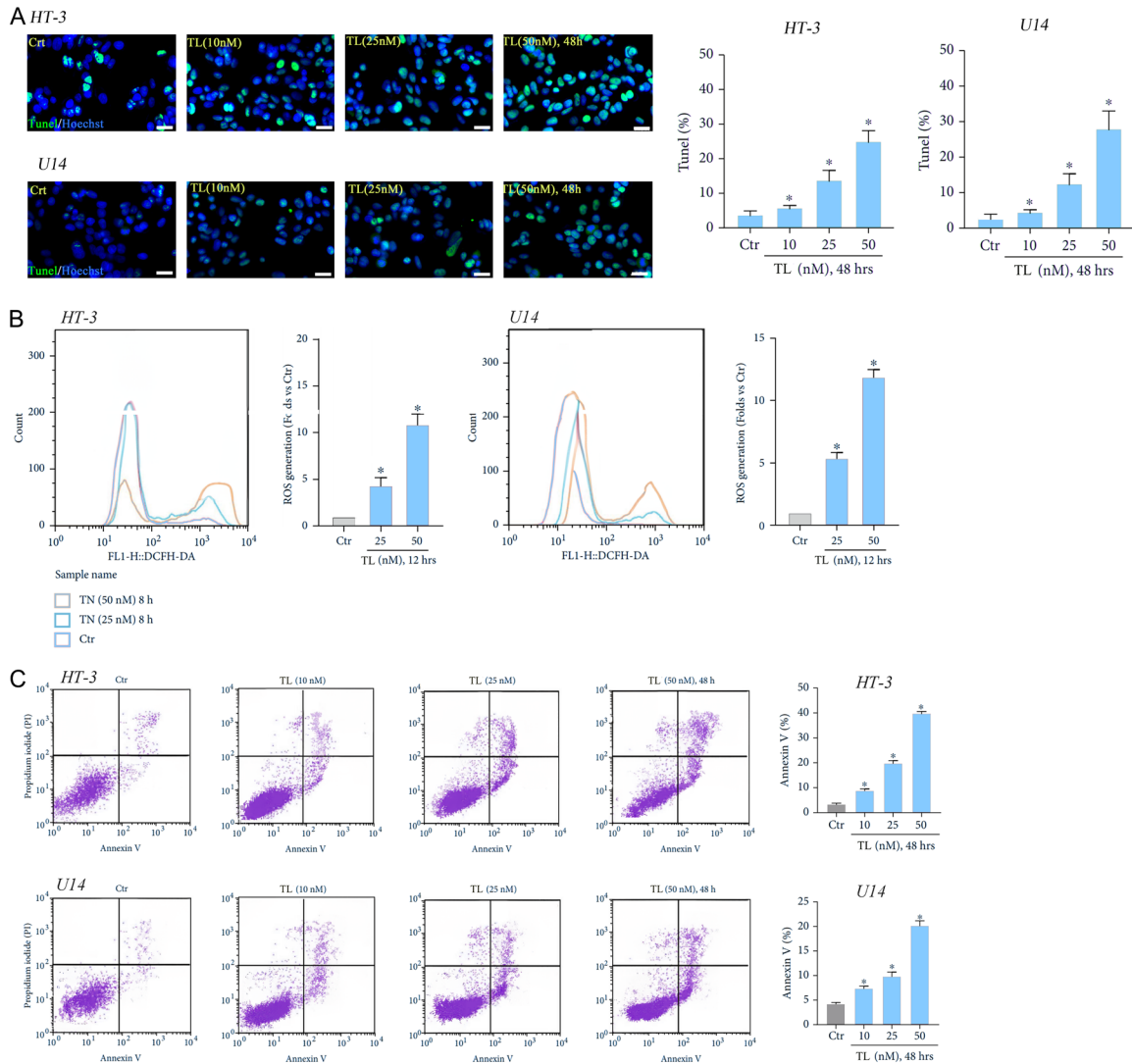


**Figure 3.** Triptonide induced apoptosis and reactive oxygen species (ROS) production in cervical cancer cells. A. TUNEL assay of HT-3 and U14 cells treated with TL (10, 25, and 50 nM) for 48 h. Scale bar, 100  $\mu$ m. TUNEL-positive cells (green) and DAPI-stained nuclei (blue) were visualized, and the percentage of TUNEL-positive cells was quantified. B. Measurement of ROS levels in HT-3 and U14 cells treated with TL (25 and 50 nM) for 12 h using the DCFH-DA probe. The fluorescence intensity was quantified to determine ROS production. C. Annexin V-FITC/PI staining and flow cytometry analysis of HT-3 and U14 cells treated with TL for 48 h. The dot plots and the percentage of Annexin V-positive cells are shown. Data are presented as the mean  $\pm$  SD. \* $P < 0.05$ , compared to the control “Ctr”.

study (**Figure 4D**), In addition, there was no significant difference in body weight between the two groups of mice throughout the study, and the tumor-to-body weight ratios were similarly visible (**Figure 4E, 4F**), suggesting that the TL treatment was well tolerated.

### *Triptonide induced immunogenic cell death in human cervical cancer cells*

Components of the endoplasmic reticulum (ER) stress response pathway have been identified

as clinically relevant drug targets that trigger immunogenic cell death (ICD), which releases vital immune stimuli or danger signals that ultimately drive effective antitumor immunity [16]. The exposure or release of damage-associated molecular patterns (DAMPs), such as ATP, high mobility group box 1 (HMGB1), and calreticulin (CRT), from cancer cells is associated with the occurrence of ICD [17]. To clarify whether TL could induce an ICD response in cervical cancer cells, we analyzed the expression of CRT and HMGB1 using Western blotting. The results

## Triptonide induces ICD in cervical cancer

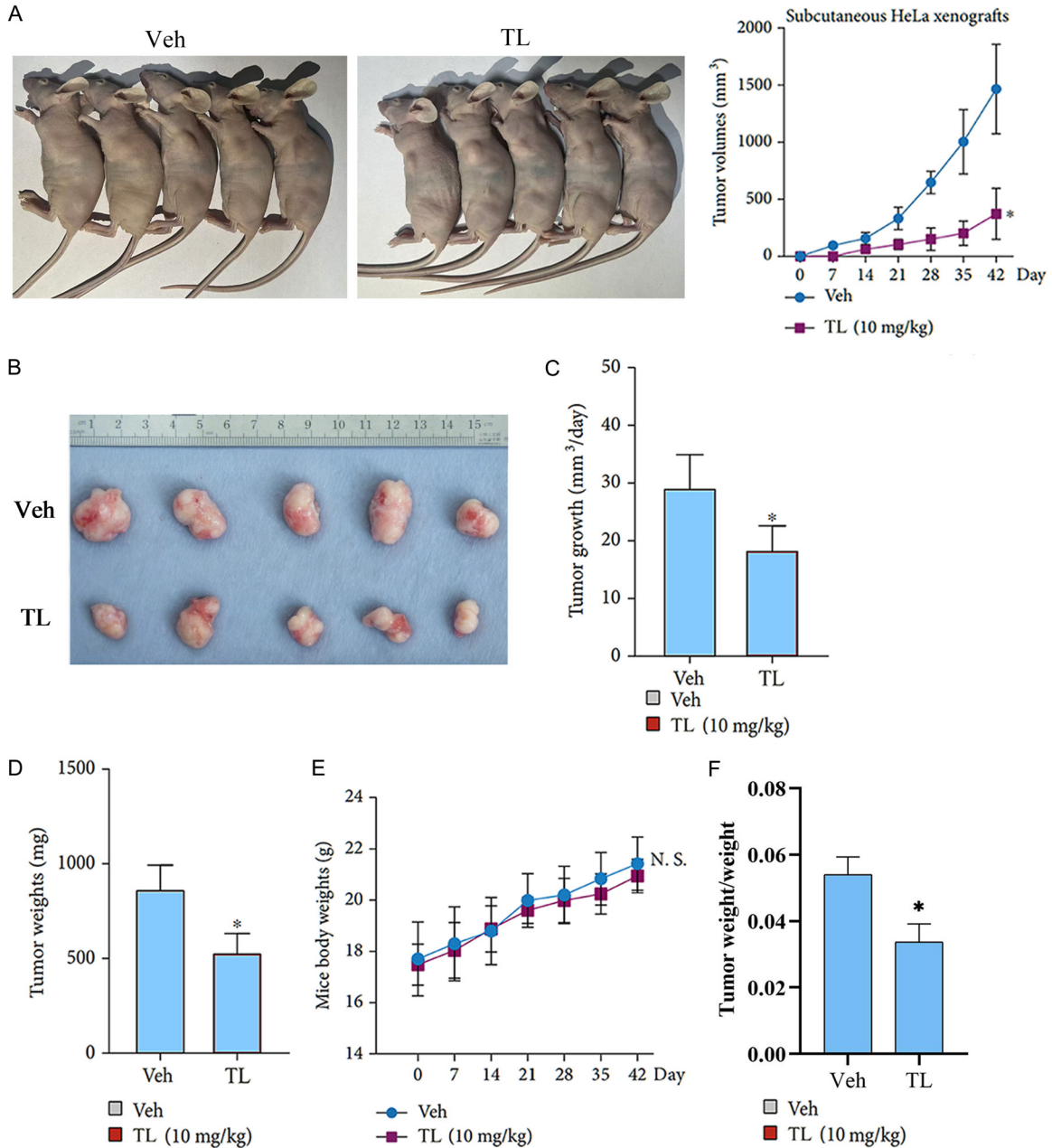


**Figure 4.** Triptonide suppressed the growth of human cervical cancer xenografts in nude mice. A. Tumor growth curves of HeLa xenografts in nude mice treated with TL (10 mg/kg, daily by gavage) or vehicle control (saline) for 21 days. Tumor volumes were measured every seven days. Scale bar, 20  $\mu$ m. B. Representative images of the excised tumors at the end of the study (day 42). C. Estimated daily tumor growth rates ( $\text{mm}^3/\text{day}$ ) of the TL-treated and control groups. D. Weight of resected tumor at the end of the study (Day 42). E. Body weights of the mice throughout the study. F. Tumor weight to body weight ratio. Data are presented as the mean  $\pm$  SD. \* $P < 0.05$ , compared to the vehicle control "Veh". N.S., not significant.

showed that CRT and HMGB1 expression was increased in HT-3 and U14 cells after TL treatment (Figure 5A). Moreover, immunofluorescence staining confirmed that CRT was increased and translocated to the surface of the

cell membrane (Figure 5D). In addition, we analyzed the extracellular content of HMGB1 and ATP in both cervical cancer cell lines. The results showed that extracellular HMGB1 and ATP levels were increased in cells treated with

## Triptonide induces ICD in cervical cancer

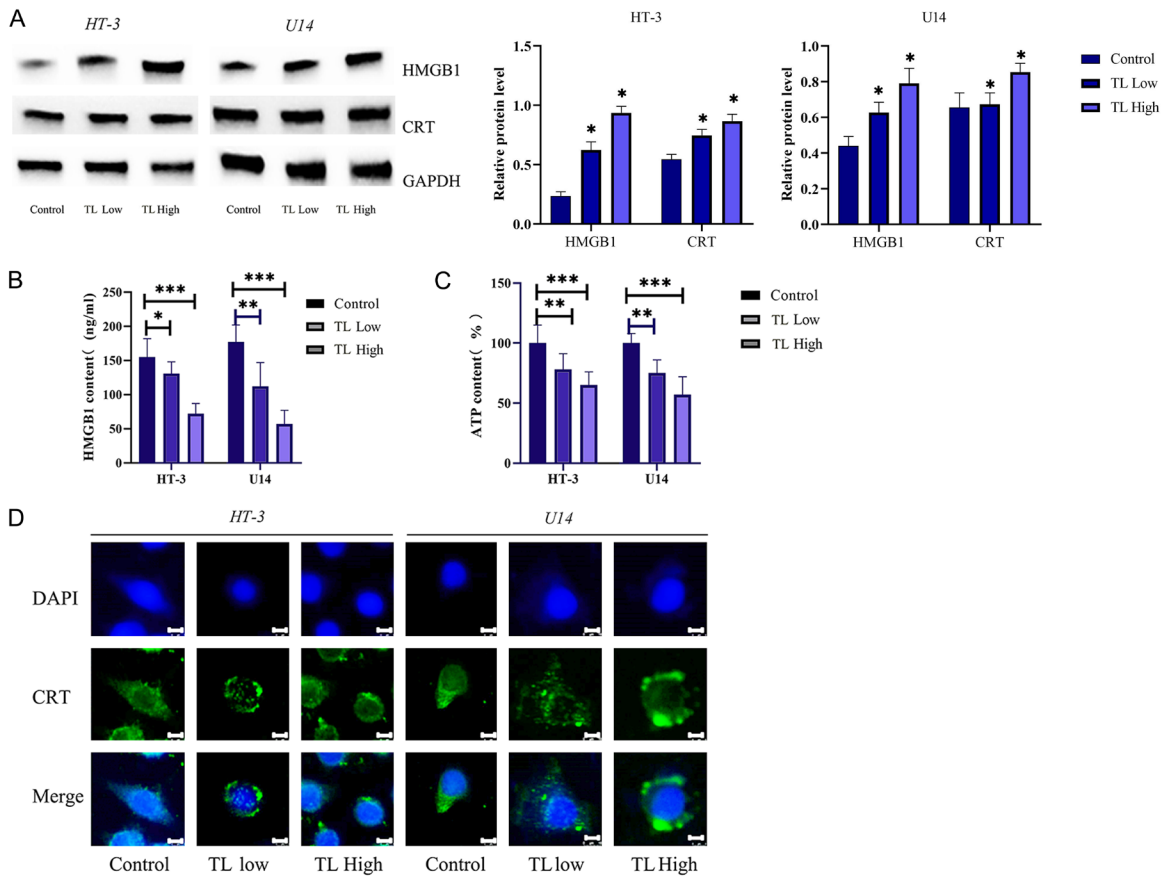


**Figure 5.** Triptonide induced immunogenic cell death in human cervical cancer cells. A. Western blot analysis of calreticulin (CRT), HMGB1, and GAPDH expression in HT-3 and U14 cells treated with vehicle control or low and high concentrations of TL for 48 h. B. ELISA measurement of extracellular HMGB1 levels in TL-treated HT-3 and U14 cells. C. Luminescence assay for the quantification of extracellular ATP levels in TL-treated cells. D. Immunofluorescence staining of CRT (green) and nuclei (DAPI, blue) in cells treated with vehicle control or TL. Merged images show the localization of CRT. Scale bar, 10  $\mu$ m. Data are presented as the mean  $\pm$  SD. \* $P$  < 0.05, \*\* $P$  < 0.01, \*\*\* $P$  < 0.001, compared to the control group.

TL (**Figure 5B, 5C**). Collectively, these data indicate that TL might induce DAMP release and cause ICD in human cervical cancer cells.

### *Triptonide-induced CRT exposure was mediated by ER stress*

To investigate the potential mechanism underlying TL-induced CRT exposure, we examined the role of ER stress. Flow cytometry analysis revealed that treatment with thapsigargin (TG), a known ER stress inducer, significantly increased the surface exposure of CRT in cervical cancer cells (**Figure 6A**), suggesting that ER stress plays a key role in translocating CRT from the cytoplasm to the cell membrane. Western blot analysis further confirmed that both TG and TL treatments upregulated the

expression of ATF3 and IRE1 $\alpha$ , upstream markers of ER stress (**Figure 6B**). We further explored the mechanism by which TL induces ER stress using bioinformatics methods. KEGG pathway enrichment analysis showed that a substantial number of differentially expressed genes (DEGs) were enriched in ROS-related pathways (**Figure 6C**). Accordingly, biological pathways such as 'detoxification of reactive oxygen species' and 'respiratory electron transport' were downregulated in the TL-treated group. In GO pathway analyses, we also found enrichment of DEGs in multiple oxidative stress and immune activation pathways (**Figure 6D**). These findings indicate that TL-induced CRT exposure is mediated by the activation of ER stress response in cervical cancer cells.

## Triptonide induces ICD in cervical cancer

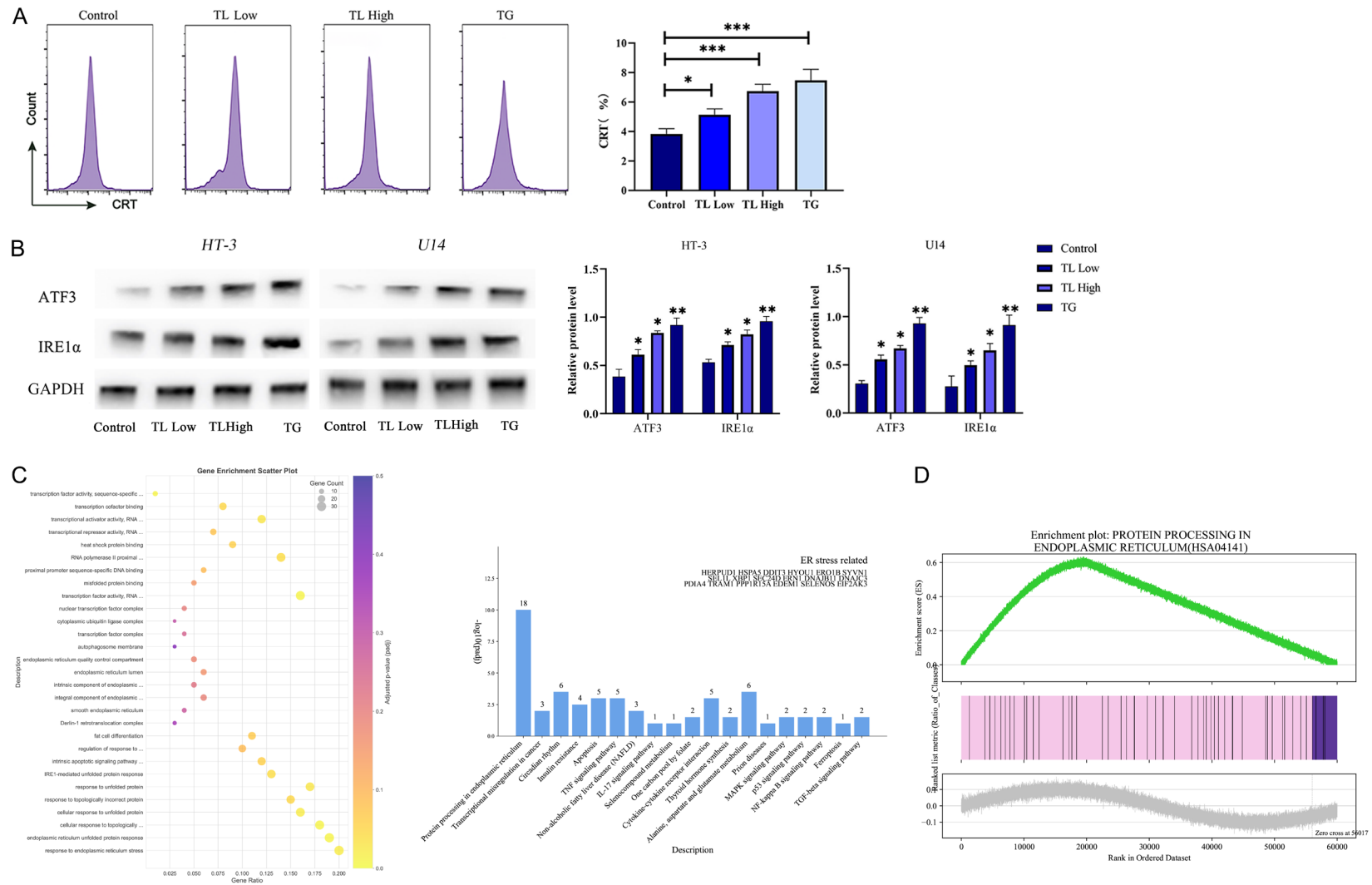


**Figure 6.** Triptonide-induced CRT exposure was mediated by ER stress. **A.** Flow cytometry analysis of surface CRT exposure in cervical cancer cells treated with TL (30 nM, low dose; 60 nM, high dose) or thapsigargin (TG, 2.5  $\mu$ M) for 24 h. **B.** Western blot analysis of ATF3, IRE1 $\alpha$ , and GAPDH expression in cells treated with TL or TG. GAPDH was used as a loading control. **C.** KEGG pathway analysis showing ROS-related pathways significantly enriched by differentially expressed genes (DEGs) upon TL treatment. **D.** GO pathway analysis highlighting the upregulation of genes involved in oxidative stress and immune response pathways following TL treatment.

### Discussion

Cervical cancer remains a significant global health burden, particularly in developing countries, despite advances in screening and prevention [25, 26]. While current treatment modalities have improved outcomes, there is an urgent need for novel therapeutic strategies to address advanced and metastatic disease [4]. In this study, we investigated the anticancer effects of TL, a key component of the Chinese herb *Tripterygium wilfordii*, on cervical cancer cells *in vitro* and *in vivo*. Our findings demonstrate that TL exhibits potent cytotoxicity, inhibits proliferation, induces apoptosis, and suppresses tumor growth in cervical cancer models. Importantly, we provide evidence that TL induces immunogenic cell death (ICD) in cervical cancer cells, suggesting its potential as an immunotherapeutic agent.

The potent cytotoxicity of TL against cervical cancer cells observed in our study is consistent with previous reports of its anticancer activity in various malignancies [1, 10, 27]. Notably, TL exerted its cytotoxic effects selectively on cervical cancer cells, as normal cervical epithelial cells were less sensitive to TL treatment. This cancer cell-specific cytotoxicity of TL is crucial for its potential clinical application, as it may minimize adverse effects on healthy tissues [13].

Cell cycle deregulation is a hallmark of cancer, and targeting cell cycle progression is a promising approach for cancer therapy [28]. Our results demonstrate that TL inhibits the proliferation of cervical cancer cells by inducing G1-S cell cycle arrest. This finding agrees with previous studies reporting TL-induced cell cycle arrest in other cancer types [29, 30]. As uncontrolled proliferation is a major driver of tumor growth and progression, the ability of TL to inhibit cervical cancer cell proliferation underscores its potential as an anticancer agent.

Apoptosis evasion is another hallmark of cancer that contributes to tumor progression and therapeutic resistance [31]. We found that TL efficiently induces apoptosis in cervical cancer cells, as evidenced by increased TUNEL-positive cells, Annexin V staining, and caspase activation. This pro-apoptotic effect of TL is consistent with previous reports in other cancer models [32]. Interestingly, we observed that TL

treatment led to increased ROS production in cervical cancer cells. ROS are known to play a crucial role in the regulation of apoptosis, and excessive ROS levels can trigger apoptotic cell death. The ability of TL to induce ROS-mediated apoptosis in cervical cancer cells suggests that redox modulation may be a key mechanism underlying its anticancer effects.

The *in vivo* anticancer activity of TL was demonstrated in a HeLa cervical cancer xenograft model. Oral administration of TL significantly inhibited tumor growth and reduced tumor burden compared to vehicle control. Importantly, TL treatment was well-tolerated, as evidenced by the lack of significant changes in body weight and the absence of overt toxicities. These findings align with previous studies reporting the *in vivo* efficacy and safety of TL in various cancer models. The potent tumor growth inhibition and favorable safety profile of TL *in vivo* support its potential for clinical translation.

One of the most significant findings of our study is the ability of TL to induce ICD in cervical cancer cells. ICD is a form of regulated cell death that elicits an immune response against cancer cells, making it an attractive strategy for cancer immunotherapy [33]. We found that TL treatment led to the exposure of calreticulin (CRT) on the cell surface and the release of HMGB1 and ATP, which are key hallmarks of ICD [14]. The translocation of CRT from the ER to the cell surface serves as an “eat me” signal for dendritic cells, facilitating the phagocytosis of dying cancer cells and the cross-presentation of tumor antigens [9]. The release of HMGB1 and ATP acts as a “find me” signal, attracting and activating dendritic cells and promoting the maturation of antigen-presenting cells [34]. These ICD-associated DAMPs play a crucial role in bridging innate and adaptive immune responses against cancer cells. The induction of ICD by TL in cervical cancer cells suggests its potential to stimulate anti-tumor immunity and enhance the efficacy of immunotherapy.

Mechanistically, we found that TL-induced CRT exposure is mediated by ER stress. ER stress is a well-established trigger of ICD, and several ER stress inducers have been shown to promote CRT translocation and ICD [35]. Our results demonstrate that TL upregulates the expression of ATF3, a key marker of ER stress, in cervical cancer cells. Moreover, bioinformat-

ics analysis revealed the enrichment of differentially expressed genes related to oxidative stress and immune activation pathways upon TL treatment. These findings suggest that TL induces ICD in cervical cancer cells through the activation of ER stress and redox modulation. Further studies are warranted to delineate the precise molecular mechanisms underlying TL-induced ICD and to evaluate its immunostimulatory effects *in vivo*.

The combination of TL with immune checkpoint inhibitors or other immunotherapeutic agents may provide a promising strategy to enhance the efficacy of cervical cancer immunotherapy. The induction of ICD by TL could potentially convert the tumor microenvironment from an immunosuppressive to an immunostimulatory state, thereby improving the responsiveness to immunotherapy. Moreover, the ability of TL to selectively target cancer cells while sparing normal tissues may help mitigate the side effects associated with current cervical cancer therapies [13]. Further preclinical and clinical studies are needed to evaluate the safety and efficacy of TL in combination with immunotherapy for the treatment of cervical cancer.

In conclusion, our study demonstrates the potent anticancer effects of TL in cervical cancer models, highlighting its ability to induce cytotoxicity, inhibit proliferation, trigger apoptosis, and suppress tumor growth both *in vitro* and *in vivo*. Notably, we provide compelling evidence that TL induces immunogenic cell death (ICD) in cervical cancer cells via the activation of endoplasmic reticulum (ER) stress and redox modulation pathways. These findings underscore the potential of TL as a novel therapeutic agent for cervical cancer and encourage further investigation into its immunomodulatory properties and potential for clinical translation. Combining TL with immunotherapy may offer a promising strategy to enhance cervical cancer treatment efficacy while minimizing adverse effects. Our study sets the stage for future preclinical and clinical research to evaluate the safety and efficacy of TL-based therapies for cervical cancer management.

### Acknowledgements

The work was supported by the Project of Jiangxi Provincial Health Commission (20221-0971), the Project of Jiangxi Provincial Admini-

stration of Traditional Chinese Medicine (2021-A100) and the Open Research Fund of Jiangxi Cancer Hospital & Institute (2021J14).

### Disclosure of conflict of interest

None.

**Address correspondence to:** Buzhen Tan, The Second Affiliated Hospital, Jiangxi Medical College, Nanchang University, No. 1 Minde Road, Nanchang 330006, Jiangxi, China. E-mail: dr\_tanbz@163.com

### References

- [1] Nisha P, Srushti P, Bhavarth D, Kaif M and Palak P. Comprehensive review on analytical and bioanalytical methods for quantification of anti-angiogenic agents used in treatment of cervical cancer. *Curr Pharm Anal* 2023; 19: 735-744.
- [2] Zeng Q, Feng K, Yu Y and Lv Y. Hsa\_circ\_0000021 sponges miR-3940-3p/KPNA2 expression to promote cervical cancer progression. *Curr Mol Pharmacol* 2024; 17: e170223213775.
- [3] Yao S, Zhao L, Chen S, Wang H, Gao Y, Shao NY, Dai M and Cai H. Cervical cancer immune infiltration microenvironment identification, construction of immune scores, assisting patient prognosis and immunotherapy. *Front Immunol* 2023; 14: 1135657.
- [4] Mayadev JS, Ke G, Mahantshetty U, Pereira MD, Tarnawski R and Toita T. Global challenges of radiotherapy for the treatment of locally advanced cervical cancer. *Int J Gynecol Cancer* 2022; 32: 436-445.
- [5] Schubert M, Bauerschlag DO, Muallem MZ, Maass N and Alkatout I. Challenges in the diagnosis and individualized treatment of cervical cancer. *Medicina (Kaunas)* 2023; 59: 925.
- [6] Song J, He GN and Dai L. A comprehensive review on celastrol, triptonide and triptonide: insights on their pharmacological activity, toxicity, combination therapy, new dosage form and novel drug delivery routes. *Biomed Pharmacother* 2023; 162: 114705.
- [7] Wang LJ, Liu Y, Li R and He DX. Metabolic analysis of triptonide microspheres in human, dog, rabbit and rat liver microsomes with UPLC-MS/MS method. *Curr Pharm Anal* 2021; 17: 1206-1217.
- [8] Hu Y, Wu Q, Wang Y, Zhang H, Liu X, Zhou H and Yang T. The molecular pathogenesis of triptonide-induced hepatotoxicity. *Front Pharmacol* 2022; 13: 979307.
- [9] Zheng B, Lu D, Chen X, Yin Y, Chen W, Wang X, Lin H, Xu P, Wu A and Liu B. Tripterygium glycosides improve abnormal lipid deposition in ne-

## Triptonide induces ICD in cervical cancer

- phrotic syndrome rat models. *Ren Fail* 2023; 45: 2182617.
- [10] Chen XL, Geng YJ, Li F, Hu WY and Zhang RP. Cytotoxic terpenoids from *Tripterygium hypoglaucum* against human pancreatic cancer cells SW1990 by increasing the expression of Bax protein. *J Ethnopharmacol* 2022; 289: 115010.
- [11] Zhan X, Zuo Q, Huang G, Qi Z, Wang Y, Zhu S, Zhong Y, Xiong Y, Chen T and Tan B. *Tripterygium glycosides* sensitizes cisplatin chemotherapeutic potency by modulating gut microbiota in epithelial ovarian cancer. *Front Cell Infect Microbiol* 2023; 13: 1236272.
- [12] Xiao Y, Yin J, Liu P, Zhang X, Lin Y and Guo J. Triptonide-induced cuproptosis is a novel anti-tumor strategy for the treatment of cervical cancer. *Cell Mol Biol Lett* 2024; 29: 113.
- [13] Zhou LN, Peng SQ, Chen XL, Zhu XR, Jin AQ, Liu YY, Zhu LX and Zhu YQ. Triptonide inhibits the cervical cancer cell growth via downregulating the RTKs and inactivating the Akt-mTOR pathway. *Oxid Med Cell Longev* 2022; 2022: 8550817.
- [14] Xu Z, Xu J, Sun S, Lin W, Li Y, Lu Q, Li F, Yang Z, Lu Y and Liu W. Mecheliolide elicits ROS-mediated ERS driven immunogenic cell death in hepatocellular carcinoma. *Redox Biol* 2022; 54: 102351.
- [15] Cai J, Zhong M, Xu J, Cheng H and Xu S. Code-livery of triptonide and IFN- $\gamma$  to boost antitumor immunity for triple-negative breast cancer. *Int Immunopharmacol* 2023; 120: 110346.
- [16] Li LB, Yang LX, Liu L, Liu FR, Li AH, Zhu YL, Wen H, Xue X, Tian ZX, Sun H, Li PC and Zhao XG. Targeted inhibition of the HNF1A/SHH axis by triptonide overcomes paclitaxel resistance in non-small cell lung cancer. *Acta Pharmacol Sin* 2024; 45: 1060-1076.
- [17] Ni X, Jiang X, Yu S, Wu F, Zhou J, Mao D, Wang H, Liu Y and Jin F. Triptonodiol, a diterpenoid extracted from *Tripterygium wilfordii*, inhibits the migration and invasion of non-small-cell lung cancer. *Molecules* 2023; 28: 4708.
- [18] Bao S, Yi M, Xiang B and Chen P. Antitumor mechanisms and future clinical applications of the natural product triptonide. *Cancer Cell Int* 2024; 24: 150.
- [19] Galluzzi L, Kepp O, Hett E, Kroemer G and Marincola FM. Immunogenic cell death in cancer: concept and therapeutic implications. *J Transl Med* 2023; 21: 162.
- [20] Sprooten J, Laureano RS, Vanmeerbeek I, Govaerts J, Naulaerts S, Borrás DM, Kinget L, Fucíková J, Špišák R, Jelínková LP, Kepp O, Kroemer G, Krysko DV, Coosemans A, Vaes RDW, De Ruysscher D, De Vleeschouwer S, Wauters E, Smits E, Tejpar S, Beuselinck B, Hatse S, Wildiers H, Clement PM, Vandenabeele P, Zitvogel L and Garg AD. Trial watch: chemotherapy-induced immunogenic cell death in oncology. *Oncoimmunology* 2023; 12: 2219591.
- [21] Li HF, Zhu N, Wu JJ, Shi YN, Gu J and Qin L. Celastrol elicits antitumor effects through inducing immunogenic cell death and downregulating PD-L1 in ccRCC. *Curr Pharm Des* 2024; 30: 1265-1278.
- [22] Shao J, Zhang C, Tang Y, He A and Zhu W. Knockdown of circular RNA (CircRNA)\_001896 inhibits cervical cancer proliferation and stemness in vivo and in vitro. *Biocell* 2024; 48: 571.
- [23] Wu W, Cheng R, Boucetta H, Xu L, Pan JR, Song M, Lu YT and Hang TJ. Differences in multicomponent pharmacokinetics, tissue distribution, and excretion of tripterygium glycosides tablets in normal and adriamycin-induced nephrotic syndrome rat models and correlations with efficacy and hepatotoxicity. *Front Pharmacol* 2022; 13: 910923.
- [24] Hatamipour M, Jaafari MR, Momtazi-Borojeni AA, Ramezani M and Sahebkar A. Evaluation of the anti-tumor activity of niclosamide nanoliposomes against colon carcinoma. *Curr Mol Pharmacol* 2020; 13: 245-250.
- [25] Narasimhamurthy M and Kafle SU. Cervical cancer in Nepal: current screening strategies and challenges. *Front Public Health* 2022; 10: 980899.
- [26] Mulongo M and Chibwasha CJ. Prevention of cervical cancer in low-resource african settings. *Obstet Gynecol Clin North Am* 2022; 49: 771-781.
- [27] Chen P, Zhong X, Song Y, Zhong W, Wang S, Wang J, Huang P, Niu Y, Yang W, Ding Z, Luo Q, Yang C, Wang J and Zhang W. Triptonide induces apoptosis and cytoprotective autophagy by ROS accumulation via directly targeting peroxiredoxin 2 in gastric cancer cells. *Cancer Lett* 2024; 587: 216622.
- [28] Xu N, Ren Y, Bao Y, Shen X, Kang J, Wang N, Wang Z, Han X, Li Z, Zuo J, Wei GH, Wang Z, Zong WX, Liu W, Xie G and Wang Y. PUF60 promotes cell cycle and lung cancer progression by regulating alternative splicing of CDC25C. *Cell Rep* 2023; 42: 113041.
- [29] Yuan C, Liao Y, Liao S, Huang M, Li D, Wu W, Quan Y, Li L, Yu X and Si W. Triptonide inhibits the progression of Glioblastoma U251 cells via targeting PROX1. *Front Oncol* 2023; 13: 1077640.
- [30] Zhang H, Mao Y, Zou X, Niu J, Jiang J, Chen X, Zhu M, Yang X and Dong T. Triptonide inhibits growth and metastasis in HCC by suppressing EGFR/PI3K/AKT signaling. *Neoplasma* 2023; 70: 94-102.
- [31] Irfan M, Javed Z, Khan K, Khan N, Docea AO, Calina D, Sharifi-Rad J and Cho WC. Apoptosis evasion via long non-coding RNAs in colorectal cancer. *Cancer Cell Int* 2022; 22: 280.

## Triptonide induces ICD in cervical cancer

- [32] Zhang H, Zhao X, Shang F, Sun H, Zheng X and Zhu J. Celastrol inhibits the proliferation and induces apoptosis of colorectal cancer cells via downregulating NF- $\kappa$ B/COX-2 signaling pathways. *Anticancer Agents Med Chem* 2022; 22: 1921-1932.
- [33] Kroemer G, Galassi C, Zitvogel L and Galluzzi L. Immunogenic cell stress and death. *Nat Immunol* 2022; 23: 487-500.
- [34] Wiernicki B, Maschalidi S, Pinney J, Adjemian S, Vanden Berghe T, Ravichandran KS and Vandenabeele P. Cancer cells dying from ferroptosis impede dendritic cell-mediated anti-tumor immunity. *Nat Commun* 2022; 13: 3676.
- [35] Zhang R, Neighbors JD, Schell TD and Hohl RJ. Schweinfurthin induces ICD without ER stress and caspase activation. *Oncoimmunology* 2022; 11: 2104551.